Hindawi
Mathematical Problems in Engineering
Volume 2019, Article ID 8262074, 11 pages
https://doi.org/10.1155/2019/8262074

Research Article

Analysis on Guide Vane Closure Schemes of High-Head Pumped Storage Unit during Pump Outage Condition

Yuquan Zhang,[1] **Yanhe Xu**,[2] **Yuan Zheng**,[1] **E. Fernandez Rodriguez**,[3] **Huiwen Liu**,[1] **and Jun Feng**[4]

[1]*College of Energy and Electrical Engineering, Hohai University, Nanjing 210098, China*
[2]*School of Hydropower and Information Engineering, Huazhong University of Science and Technology, Wuhan 430074, China*
[3]*Technological Institute of Merida, Technological Avenue, Merida 97118, Mexico*
[4]*Powerchina Zhongnan Engineering Corporation Limited, Changsha 410014, China*

Correspondence should be addressed to Yanhe Xu; yh_xu@hust.edu.cn

Received 30 August 2019; Accepted 5 December 2019; Published 31 December 2019

Academic Editor: Ricardo Perera

When the pumping operation of pumped storage unit suffers from power outage, the hydraulic transient poses a serious threat to the safe operation of the unit and its pressure pipeline system. For high-head pumped storage power station (PSPS), the water hammer pressure (WHP) and rotational speed rise ratio (RSRR) of each hydraulic unit will be increased during the pump outage condition. In order to limit the fluctuation of rotational speed and WHP in power-off condition, optimizing and choosing a reasonable guide vane closure scheme (GVCS) is an economic and efficient means to improve the dynamic characteristics of pumped storage unit. On the basis of the calculation model of the transition process of single tube-double unit type of a high-head PSPS, an optimization model of GVCS balancing WHP and RSRR objectives is established. Furthermore, the two-stage broken line and three-stage delayed GVCSs are applied to the pump outage condition, and the nondominated sorting genetic algorithm-II (NSGA-II) is introduced to calculate the optimal solution set under different water heads and different closure schemes. For four typical water heads, the multiobjective optimization results of the closure law show that the two-stage broken line law has a better Pareto front under high water head, while the three-stage delayed law has a better performance under low water head. Furthermore, through the results of transition process of typical schemes, the adaptability of GVCS and water head is analyzed. The method proposed in this paper can make the RSRR not more than −0.89, and the three-stage delayed law can even make the RSRR only −0.01. Methods of this paper provide a theoretical basis for optimum guide vane closure mode setting of PSPS.

1. Introduction

Investment in renewable energy schemes improves economic stability and reduces pollution [1]. Out of all green technologies installed in the world, hydropower remains the largest and most common [2] and competitive [3, 4]. Hydropower systems are used to store and convert potential energy into electrical energy, through pumped storage equipment [5, 6]. Given equipment is useful for solving the intermittence issues of renewable resources and is widely backed for its high capacity, reliability, and economics [7, 8]. Therefore, the larger the growth of renewable energy, the larger the need of PSPS to balance the load variation and increase the network reliability [9]. Another feature is their flexibility to make up for the stochastic of solar and wind power, which is helpful for the multienergy complement [10].

The reversible pump turbine is an important component of the PSPS which experiences different transitional processes to achieve the function of regulation by switching between turbine and pump mode [11, 12]. A conventional method to deal with the transient conditions of the pumped storage unit has been to optimize the GVCS. For instance, a nonoptimal GVCS under extreme conditions causes the WHP and RSRR to rise and exceed the allowable range of design, thus resulting in unfavorable phenomena such as overspeed of the unit, abnormal vibration, and

asynchronization of the movable guide vanes [13, 14]. This would be a serious threat to the safety of the PSPS especially when it is under the pump outage condition, since the RSRR of the unit will increase greatly and lead to the significant change of flow rate, increasing the WHP. The stable and safe operation of the unit will be affected if no actions are taken. The guide vanes are often required to close or open at a certain rotational speed in these transient processes, resulting in dynamic instabilities and damaging the hydraulic system. Therefore, the flow mechanism during the transient processes with the closure schemes of the guide vanes should be studied in order to reduce the adverse impact of high WHP and RSRR.

Many methods are available in the literature for improving the GVCS, in terms of stability and lifespan of the PSPS. Zeng et al. [15] investigated different GVCSs for reducing the pulsating pressures, runaway speed, and WHP; thus, the selection for two-stage GVCS during the transient process was present. Yu et al. [16] investigated different GVCSs using high-head pump-turbine load rejection process, and a novel two-stage GVCS was obtained to reduce the effects from S-shaped region. Therefore, the maximum pressure in the spiral case and rotating speed during the transient process was mitigated. Zhang et al. [17] discussed the broken line GVCS of reversible pump turbine for a certain power station, and the results indicated that WHP caused by wicket gate closing together with RSRR was effectively decreased. However, it was shown that two-stage GVCS was weak in reducing the WHP and RSRR during load rejection and pump outage condition. Kuwabara et al. [18] proposed a new control method, and computer simulation on the curved closure scheme showed a reduction of the penstock design pressure and the WHP; therefore, the operating point was prevented from the effects of S-shaped characteristics. However, the curved closure scheme was difficult to obtain as it had a high requirement on the servomotor. Additionally, the method of misaligned guide vane has been applied to reduce the WHP of the unit in the S-shaped region [19]. On the downside, the previous method increases the hydraulic system oscillations and has a negative impact on the operation of the power plant [20]. Therefore, theoretical analyses and optimal closure schemes are required to reduce the WHP and RSRR and thus improve the stability of the pumped storage unit especially during pump outage condition.

Due to the complicated and multiobjective nature of the guide vane flow, the optimization process requires fast and intelligent solutions, such as the particle swarm optimization (PSO), gravitational search algorithm (GSA), and nondominated sorting genetic algorithm (NSGA) [21–25]. The NSGA proposed in [26] was one of the first evolutionary algorithms to obtain multiple Pareto-optimal solutions in one single simulation run. However, NSGA is computationally expensive for large population sizes and requires the specification of a sharing parameter. Compared with the NSGA algorithm, the NSGA-II algorithm [27] adopts the fast nondominated sorting method, which greatly reduces the computational complexity and maintains the diversity of the population effectively. Cases of complex extreme operating conditions of single tube-double unit type pumped storage units systems were studied to verify the feasibility and effectiveness of the proposed NSGA-II in solving optimization of GVCS.

The remaining part of this paper is organized as follows. Section 2 establishes a mathematical model of pumped storage unit. In Section 3, multiobjective genetic algorithm and optimization method of GVCS is introduced simultaneously. In Section 4, the optimization cases of GVCS under four typical water heads are introduced and the applicability and advantages of the two closure methods for each water head are discussed. The conclusions are summarized in the Section 5.

2. Mathematical Model of Pumped Storage Unit

2.1. Method of Characteristics. The transient process model of pumped storage unit was solved by using the method of characteristics, and the basic motion and continuity equation of unsteady flow in pressurized pipeline are shown below [28–32].

$$\text{Motion equation: } \frac{\partial V}{\partial t} + V\frac{\partial V}{\partial x} + g\frac{\partial H}{\partial x} + \frac{f}{2D}V|V| = 0,$$
$$\text{continuity equation: } \frac{a^2}{g}\frac{\partial V}{\partial x} + V\left(\frac{\partial H}{\partial x} + \sin\alpha\right) + \frac{\partial H}{\partial t} = 0, \tag{1}$$

where V represents the velocity of flow, H, the head of the pressure measuring pipe, f, the friction coefficient, a, the water hammer velocity, D, the diameter of the pipe, α, the angle between the line of the shape center of pipe each section and the horizontal plane, and g, the gravitational acceleration. V and H are functions of time t and pipe length x, respectively.

The method of characteristic was applied to solve the above equations. Then, these were transformed into simplified equations set up on the characteristic line $dx/dt = \pm a$, as shown in equations (2) and (3):

$$C^+: \begin{cases} \dfrac{dH}{dt} + \dfrac{a}{gA}\dfrac{dQ}{dt} + \dfrac{af}{2gDA^2}Q|Q| = 0, \\ \dfrac{dx}{dt} = a, \end{cases} \tag{2}$$

$$C^-: \begin{cases} \dfrac{dH}{dt} - \dfrac{a}{gA}\dfrac{dQ}{dt} - \dfrac{af}{2gDA^2}Q|Q| = 0, \\ \dfrac{dx}{dt} = -a, \end{cases} \tag{3}$$

where A is the pipe cross section area and Q is the cross section flow of pipeline. The surge chamber, ball valve, and bifurcation pipe were treated as boundary conditions, and the first-order inertia model was adopted for the generator motor model.

2.2. Parameters of Pumped Storage Unit. The full characteristic curve data and related parameters of water diversion pipeline used in the calculation model of pumped storage unit during transition process were consistent with the

actual physical parameters of the PSPS located somewhere in China. Table 1 shows the physical parameters of the power station whist Figure 1 presents the full characteristic data of the pump turbine.

2.3. Model of Motor. In this paper, because only the unit speed changes are considered, the dynamic equation of the motor taking account of speed characteristic is simplified to a first-order equation as follows:

$$G(s) = \frac{x(s)}{e(s)} = \frac{1}{T_a s + e_g}, \tag{4}$$

where x is the pump-turbine speed relative deviation, e is the error between system input and output, T_a is the inertia time constant of the motor, e_g is the adjusting coefficient of the motor, and s is the Laplace operator.

3. Multiobjective Genetic Algorithm and Optimization of GVCS

3.1. Multiobjective Genetic Algorithm. The algorithmic model NSGA-II is divided into three steps: population stratification, congestion calculation, and generation evolution [33].

3.1.1. Population Stratification. In the minimization objective function $y(x) = (f_1(x), f_2(x), \ldots, f_n(x))$, the population size is assumed to be m.

(1) Firstly, $i = 1$, $j = 1, 2, 3, \ldots, m$, and $j \neq i$ are set.

(2) P_o is the number of dominating individuals o in the population. nPop is the population size; pc is the crossover; pm is the mutation ratio; mu is the mutation rate; sig is the mutation step; and MI is the maximum iteration number. The dominance relation between solutions x_i and x_j is compared. When x_i dominates x_j, x_j is placed into the set of S_i and there is an index relationship between the set Si and xi. When x_i is dominated by x_j, P_{x_i} is set as $P_{x_i} = 1$. Then, i is set as $i = 2$, and the above steps are repeated until all the solutions in the population are compared and the number of individuals dominating other solutions and the set of solutions dominated by each solution are obtained.

(3) All solutions of $P_o = 0$ in the population are found and placed into the set of F_1. In other words, the hierarchies of all individuals in the set of F_1 are 1.

(4) F_1 is taken as the current set, and each individual h is put in the set F_1 whose dominant individual set is S_h. P_c is the capacity of elite archive set. Each individual c in the set S_h is executed as $P_c = P_c - 1$, and the dominant individual solution c is reduced by one. If $P_c = 0$, the individual c is put into the set F_2, and all individual hierarchies in the set F_2 are equal to 2. Then, the above steps with F_2 as the current set are repeated.

(5) The iteration will be completed until the entire population is stratified.

Table 1: Physical parameters of the PSPS.

Runner diameter (m)	Rated rotational speed (r/min)	Rated flow rate (m^3/s)	Rated head (m)	Rated power (MW)
3.85	500	62.09	540	306

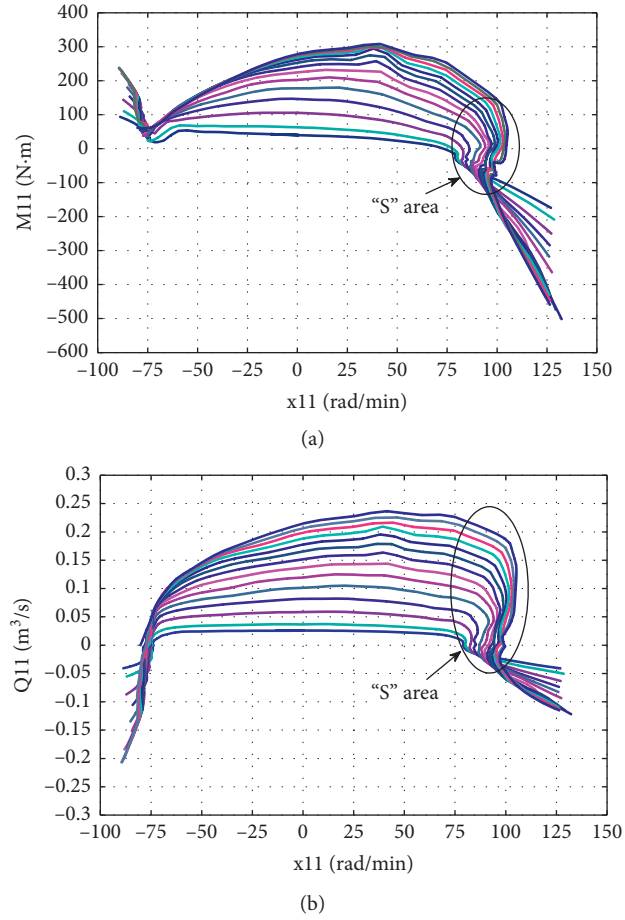

Figure 1: The full characteristic data of the pump turbine. (a) Torque. (b) Flow rate.

3.1.2. Congestion Calculation. At the same level, in order to get the best solution and ensure the diversity of the population, it is necessary to introduce the congestion degree calculation m_d. The population is sorted based on the objective function of each unit. For boundary individuals, the congestion degree of the first and last individual is set to infinite. The other individual congestion calculation formula is indicated as follows:

$$m_d = f_n(i+1) - f_n(i-1). \tag{5}$$

3.1.3. Generation Evolution. The genetic and mutation derived offspring population and the paternal population are combined into a new population to find the optimal solution in the new population.

3.2. Objective Function for Optimization of GVCS. During the pump outage condition of the pumped storage unit, the WHP and RSRR are the key indicators to measure the safe and stable operation of the unit. For this reason, the WHP and RSRR are taken as the objective functions for the optimization of GVCS [34].

3.2.1. Water Hammer Pressure. It is a complex condition for the pumped storage unit during pump outage condition. In order to obtain the pressure of each hydraulic unit, the WHP of volute, draft tube, and the constraint of surge water level were taken into account as shown in the following equation:

$$\text{Min Obj}_{\text{pre}} = u_a \sum_{i=1}^{N} \left(f_{\text{vol}} + f_{\text{dra}}\right) + u_b\left(L_{\text{up}} + L_{\text{dow}}\right), \quad (6)$$

where f_{vol} is the maximum pressure at the end of volute of unit i; f_{dra} is the maximum pressure at the inlet of draft tube of unit i; L_{up} is the maximum surge water level in upstream surge tank; L_{dow} is the maximum surge water level in downstream surge tank; and u_a and u_b are the characteristic coefficients of WHP and water level in the surge tank, respectively.

3.2.2. Rotational Speed Rise Ratio. RSRR is caused by the unbalanced energy between the turbine and the generator when the load rejection or pump outage occurs, which makes the rotational speed of the pumped storage unit change. The percentage of the change of the unit speed to the rated speed is defined as RSRR. Taking the unit 100% load rejection as the precondition, the calculation formula of RSRR is defined as

$$\text{Min Obj}_{\text{spe}} = \left(1 + \frac{365 N_0 T_s f_c}{n_0^2 G D^2}\right)^{0.5} - 1, \quad (7)$$

where N_0 is the load at the beginning of the unit; T_s is the duration from full opening to no load, which is mainly determined by the guide vane closure time; n_0 is the initial rotational speed of the unit; G is the weight of the rotating part of the unit; D is the inertial diameter; combined GD^2 constitutes the unit's rotational inertia; and f_c is the correction coefficient. As observed in equation (7), the longer the guide vane closure time, the higher the speed rise rate of the unit.

In the intelligent algorithm model, $\text{Min Obj}_{\text{pre}}$ and $\text{Min Obj}_{\text{spe}}$ are the two optimization objectives of GVCS.

3.3. Description of GVCS

3.3.1. Two-Stage Broken Line Closure Scheme. The two-stage broken line GVCS is divided into two stages from the original opening to the full closure state at two different closing rates. Therefore, due to the different speed of the two stages, the two-stage broken line closure scheme can be divided into two modes of "fast followed by slow" and "slow followed by fast," as shown in Figure 2.

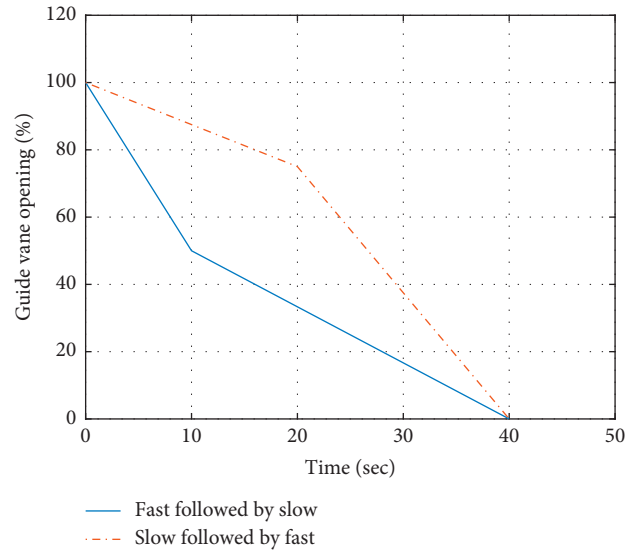

Figure 2: Two-stage broken line GVCS.

For the two-stage broken line GVCS, the optimization consists in choosing the closing speed of the guide vane in the first and second stages and selecting the position of inflection point. Because of the large optimization space of the two-stage broken line GVCS, this method meets the constraints of most PSPS and thus the reason for its high usage in variety of applications.

3.3.2. Three-Stage Delayed Closure Scheme. The three-stage delayed GVCS generates from the two-stage broken line GVCS. For three-stage delayed GVCS, different problems and conditions will lead to changes in the time period of delayed closure. The three-stage delayed GVCS is shown in Figure 3.

In order to limit the maximum WHP, the guide vane is delayed closed when the unit working condition is close to the S-shaped region; therefore, the closure of the guide vane and the change of rotating speed will have less effect on the flow rate, thus reducing the maximum pressure.

For three-stage delayed closure of guide vanes, the optimization space is very large. The closing speed of the first and second guide vanes' closure and the closing time of the delay period can be optimized. Therefore, the three-stage delayed GVCS can be applied to most of the PSPS. Based on practical engineering experience, this paper takes the speed reaching a certain threshold as the criterion, and the delay time is 3 to 7 seconds.

3.4. Optimization of GVCS. In the PSPS, the selection of GVCS is a convenient and effective measure to ensure the safe and stable operation of units. The optimization of GVCS is also the optimization of turbine unit transition process. Therefore, the optimization of GVCS has great significance for PSPS. When calculating the GVCS during the transient process, the parameters of the simulation model should be consistent with the actual parameters of the PSPS so as to improve the practicability and accuracy of the calculation

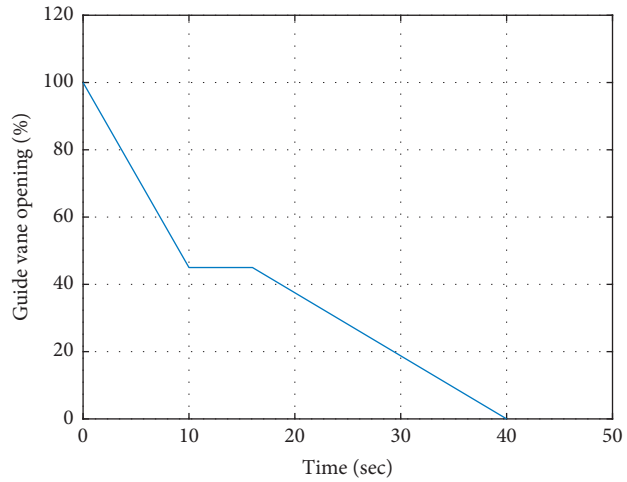

Figure 3: Three-stage delayed GVCS.

model for GVCS. Generally, the calculation model of GVCS mainly considers two objectives: WHP and RSRR. Therefore, the calculation model of GVCS needs to satisfy the constraints of WHP and RSRR of the system. The process of optimization of GVCS problem solving with multiobjective genetic algorithm is illustrated in Figure 4.

On this basis, the optimization goal is achieved by changing the closing speed of guide vane, i.e., the effective closing time of guide vane and the position of inflection point. For the two target values of WHP and RSRR, the weight method is usually used to construct the function and complete the solution. However, the selection of weight coefficients needs to be analyzed according to the actual situation of PSPS, and the weight coefficients need to be calculated strictly. Otherwise, the optimization results obtained from simulation may not conform to the actual situation, thus impairing the safe and stable operation of the unit.

4. Case Study

4.1. Parameters of Numerical Experiments. The simulation parameters were set as follows: the population size *nPop* was 80; the crossover ratio *pc* was 0.7; the mutation ratio *pm* was 0.4; the mutation rate *mu* was 0.02; the mutation step *sig* was 0.1; the maximum iteration number *MI* was 200; the simulation time step length was 100 s; and the interval time was 0.04 s.

For the single tube-double unit type unit, this paper studied the schemes under different water heads. The setting conditions and heads in pump outage condition are shown in Table 2.

4.2. Simulation Results of Pump Outage Condition. During the pump outage condition of the pumped storage unit, four typical heads shown in Table 2 were taken for simulation. The transition process of the unit was calculated by using two-stage broken line and three-stage delayed GVCS, respectively. Based on the constraint condition of GVCS, the multiobjective genetic algorithm NSGA-II was

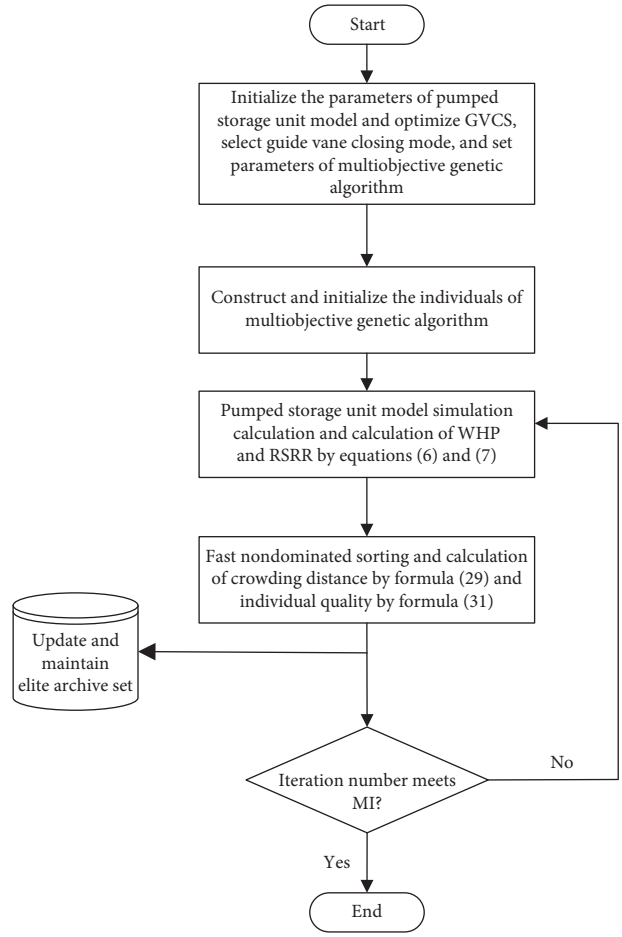

Figure 4: Process of optimization of GVCS with multiobjective genetic algorithm.

used to optimize the solution set with the target of minimum WHP and RSRR. The result of Pareto front of WHP as abscissa and RSRR as ordinate was obtained.

4.2.1. Results of Two-Stage Broken Line Closure Scheme. In the optimization calculation model of GVCS, under four water heads, the results of WHP as abscissa and RSRR as ordinate are obtained by using two-stage broken line GVCS, as shown in Figure 4.

In Figure 5, for the two-stage broken line GVCS, the unit has a better Pareto frontier set when operating at Head 1 and Head 3. Specifically, the WHP of Head 1 is smaller than Head 2, Head 3, and Head 4 for the same RSRR. When the WHP is approximately the same and is lower than 3650 m H_2O, Head 3 has a smaller RSRR compared with Head 2 and Head 4. It can be seen that there is little difference between the WHP and RSRR of Head 2 and Head 4. Therefore, the two-stage broken line closure scheme of guide vane is more suitable for the working condition of high water head range.

4.2.2. Results of Three-Stage Delayed Closure Scheme. In the optimization calculation model of GVCS, the Pareto frontier

Table 2: The setting condition parameters during pump outage condition.

Water head	Upper level (m)	Lower level (m)	Load variation	Description of water level combination and guide vane closure scheme
Head 1	735.45	163.00	100% ⟶ 0	The upper level is the level of check flood while the lower level is the level of dead water. The guide vanes are closed normally.
Head 2	735.45	181.00	100% ⟶ 0	The upper level is the check flood level, and the lower level is the normal water level. The guide vanes are closed normally.
Head 3	733.00	163.00	100% ⟶ 0	The upper level is the normal water level, and the lower level is the dead water level. The guide vanes are closed normally.
Head 4	733.00	181.00	100% ⟶ 0	The upper level is the normal water level, and the lower level is the normal water level. The guide vanes are closed normally.

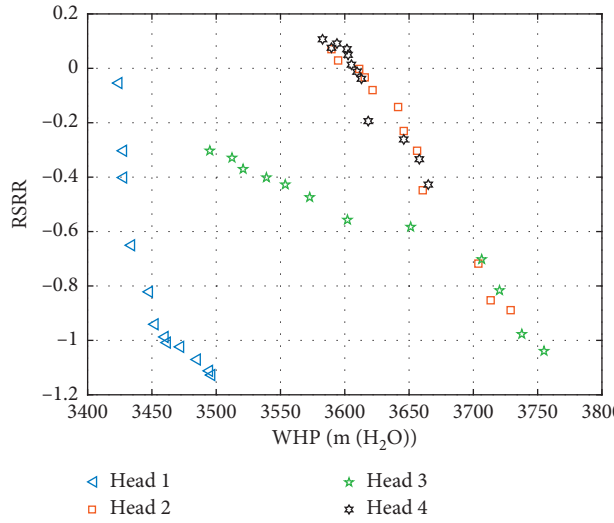

Figure 5: Pareto frontier sets of two-stage broken line GVCS under four heads.

set under four heads is obtained by using three-stage delayed GVCS, as shown in Figure 6.

In Figure 6, with approximately the same condition of RSRR, WHP of Head 3 is smaller than Head 2, Head 1, and Head 4, while the RSRR and WHP of Head 1, Head 2, and Head 4 are similar. Therefore, the three-stage delayed GVCS has relatively universal adaptability to the four water heads and is more suitable for the working condition of Head 3.

4.2.3. Results of Different GVCSs under Different Water Heads. Under four water heads, the optimization results of different GVCSs are compared, and the results of WHP and RSRR were obtained as follows.

Figure 7 shows the relationship between WHR and RSRR for the two-stage broken line and the three-stage delayed GVCS. From the above four contrast diagrams, it can be seen that the two-stage broken line GVCS is better than the three-stage delayed closure scheme in optimizing the WHP and RSRR for Head 1. Therefore, the two-stage broken line GVCS is more suitable for the Head 1 under the

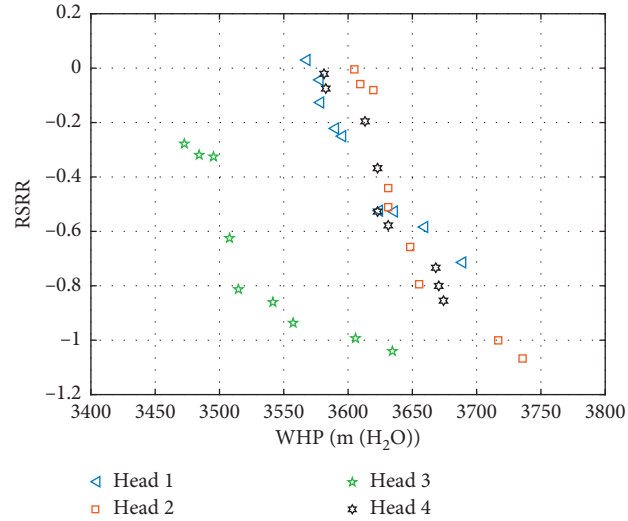

Figure 6: Pareto frontier sets of three-stage delayed GVCS under four heads.

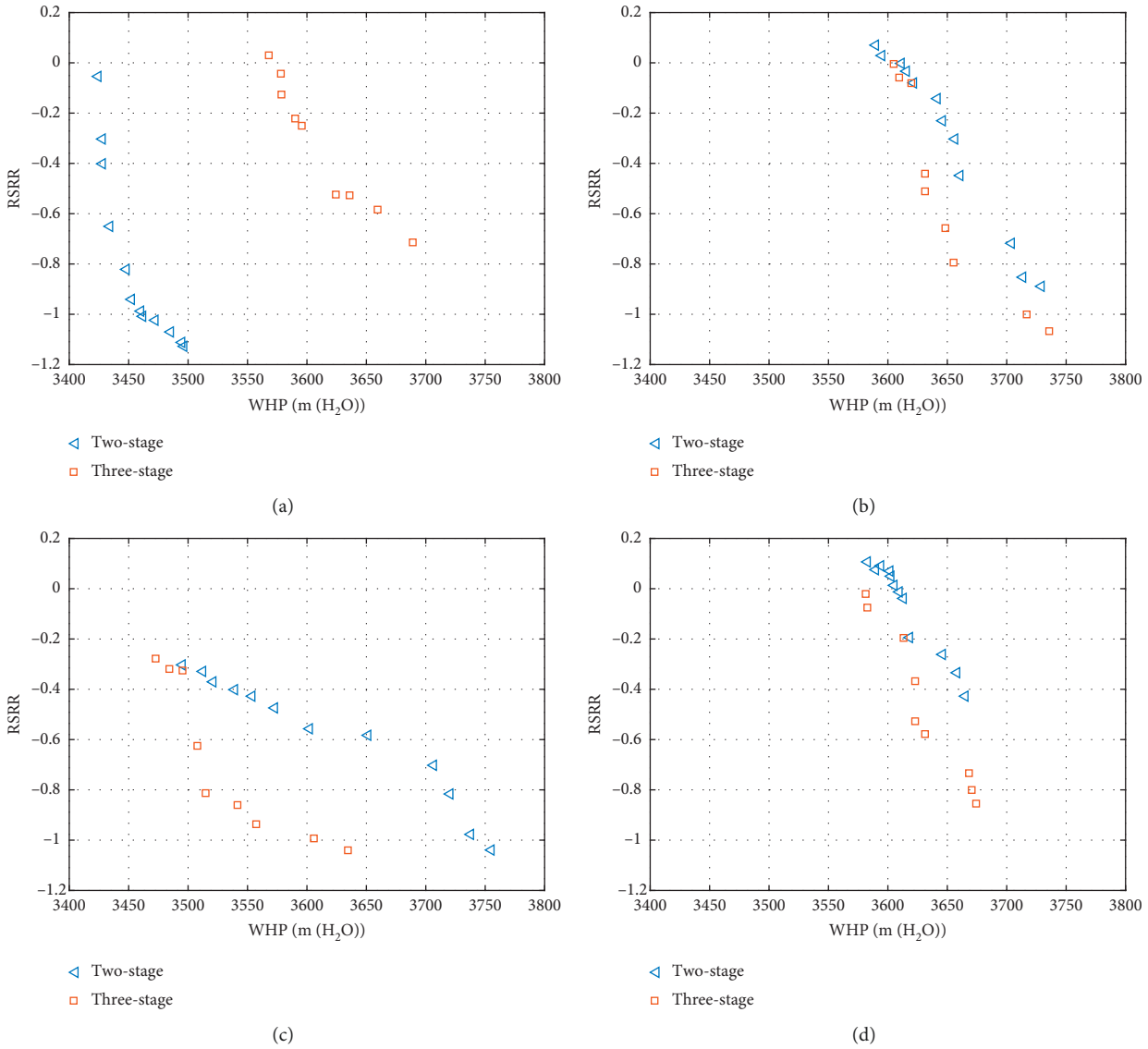

Figure 7: Comparison of Pareto frontier sets under different water heads. (a) Head 1. (b) Head 2. (c) Head 3. (d) Head 4.

pump outage condition for high-head PSPS. In the case of Head 2, Head 3, and Head 4, the WHP of three-stage delayed GVCS is lower than that of two-stage broken line closure scheme.

To further verify the validity of the model of GVCS, the two-stage broken line GVCS in Head 1 mode and the three-stage delayed GVCS in Head 4 mode were taken for simulation. Then, the indicator values in the transition process calculation of the schemes with minimum WHP and RSRR were obtained, respectively.

For the model of two-stage broken line GVCS of Head 1, the constraints of minimum WHP and RSRR are listed as in Table 3, whilst Figure 8 compares the schemes based on the minimum WHP and RSRR of the transition process.

For the model of three-stage delayed GVCS of Head 4, the constraints of the minimum WHP and RSRR are listed as in Table 4, and the schemes based on the minimum WHP and RSRR of the transition process are compared in Figure 9. It can be clearly seen that the three-stage delayed GVCS has a good optimization effect for the WHP and RSRR, the hydraulic factors meet the safety requirements of the project, and the RSRR range is only −0.01~−0.81, which significantly improves the mechanical and hydraulic stability of the unit operation.

The simulation results of transition process on three-stage delayed GVCS of Head 4 are shown in, Figure 9.

In Figure 9, the comparison of three-stage delay GVCS under head 4 shows that in the process of closure of guide vanes under Min. RSRR scheme, the unit speed does not enter the threshold of "S" region, so it does not need a long time delay closure to meet the constraints. In Min. WHP scheme, if the unit speed reaches the threshold of "S" region, the guide vane of the unit will be closed for 3–7 seconds, which can rapidly reduce the rise of WHP.

From above results, it can be seen that the GVCS during pump outage condition in high-head PSPS has a significant effect on reducing the WHP and RSRR.

Table 3: Index data of minimum WHP and RSRR under the two-stage broken line GVCS of Head 1.

	Max. volute pressure	Max. draft tube pressure	Max. speed rise	Upstream surge tank		Downstream surge tank	
				Max.	Min.	Max.	Min.
Min. WHR	679.42	113.21	−0.89	740.49	721.52	190.89	171.54
Min. RSRR	751.74	111.30	−0.23	739.75	722.33	190.73	171.72

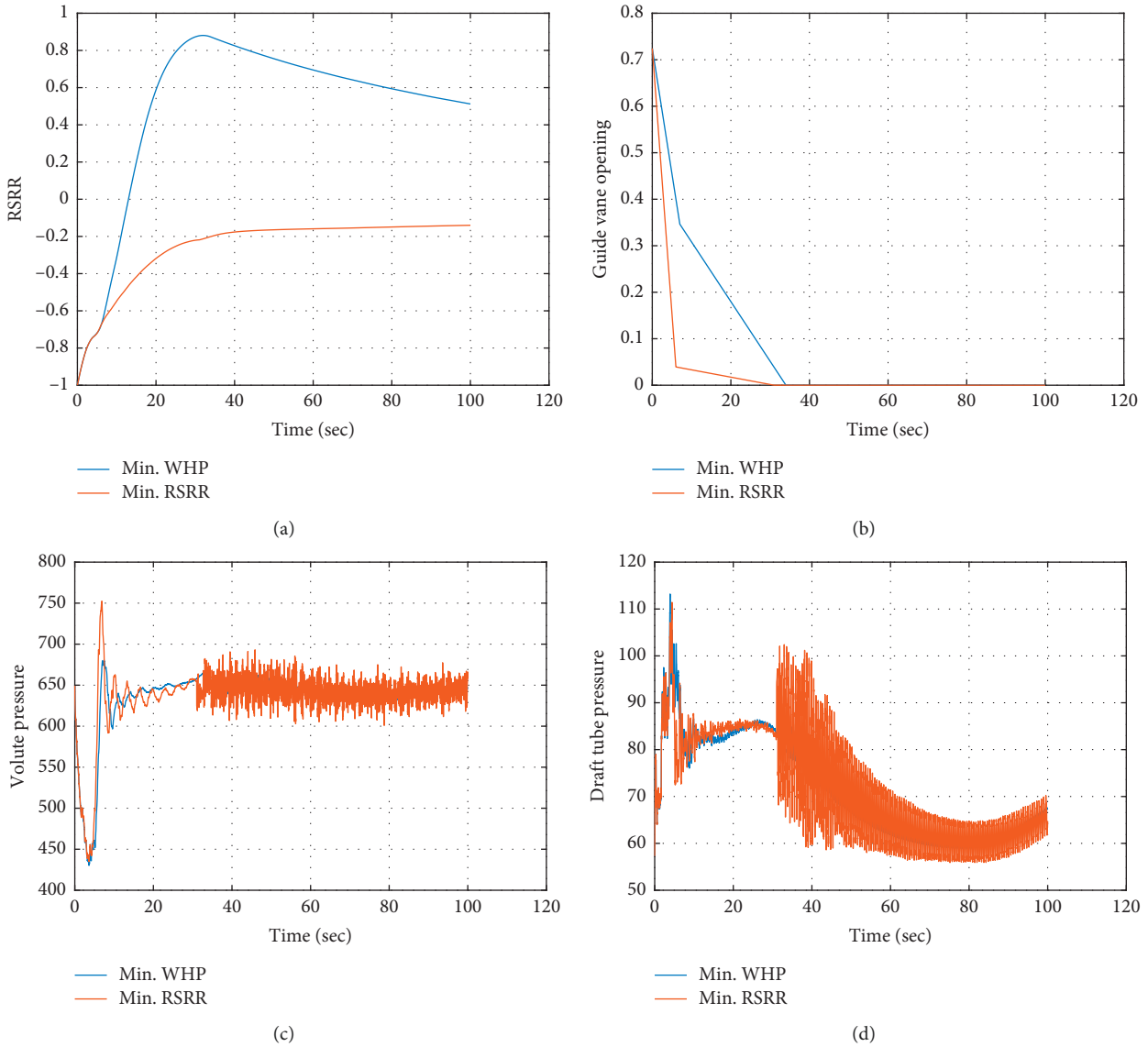

Figure 8: Simulation results of transition process on two-stage broken line GVCS of Head 1. (a) RSRR. (b) Guide vane opening. (c) Volute pressure. (d) Draft tube pressure.

Table 4: Index data of minimum WHP and RSRR under the three-stage delayed GVCS of Head 4.

	Max. volute pressure	Max. draft tube pressure	Max. speed rise	Upstream surge tank		Downstream surge tank	
				Max.	Min.	Max.	Min.
Min. WHR	690.80	121.71	−0.81	740.20	722.65	179.08	153.11
Min. RSRR	761.40	123.89	−0.01	740.05	722.26	178.74	153.33

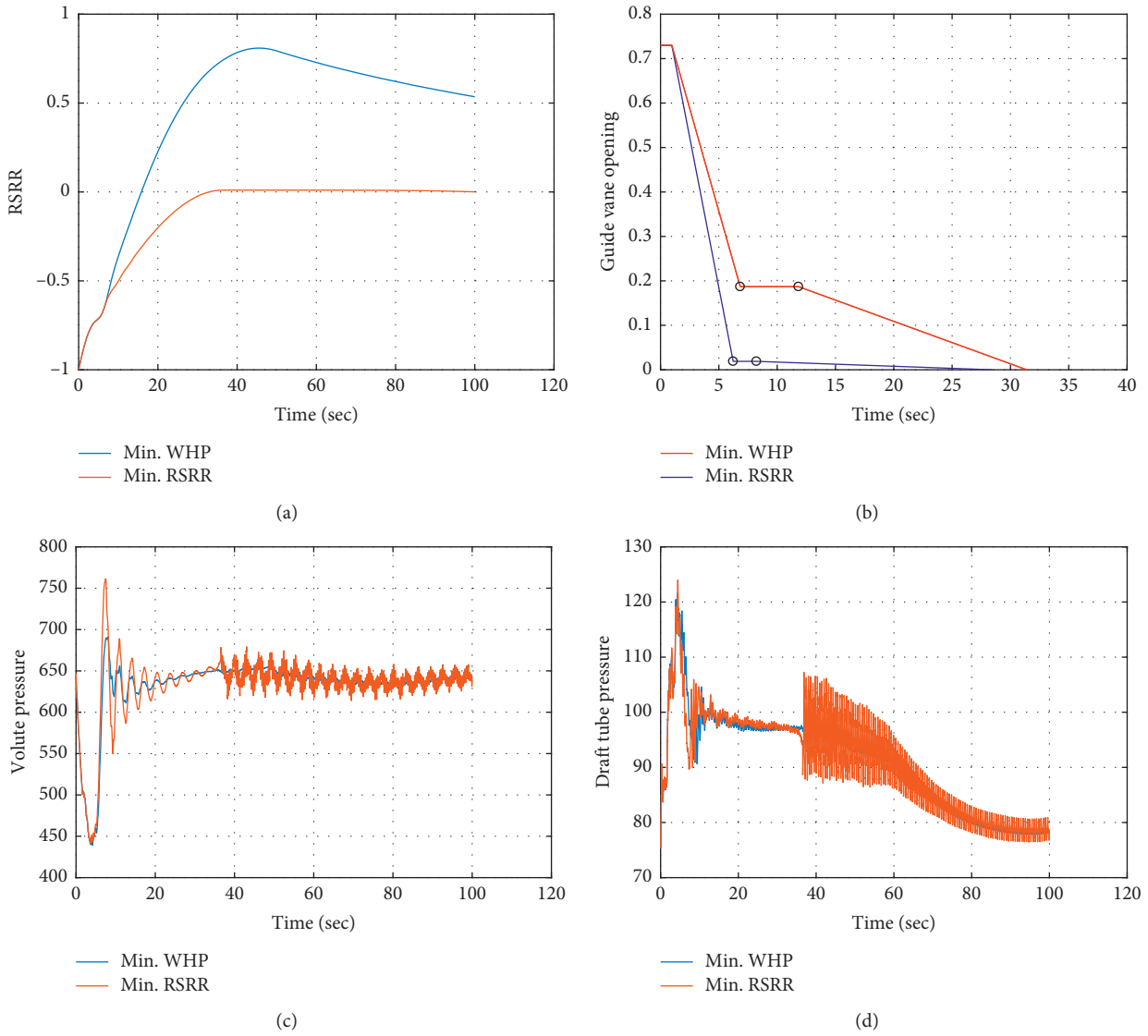

Figure 9: Simulation results of transition process on three-stage delayed GVCS of Head 4. (a) RSRR. (b) Guide vane opening. (c) Volute pressure. (d) Draft tube pressure.

5. Conclusion

In this paper, a multiobjective genetic algorithm is used to establish an intelligent algorithm optimization model of pump outage condition targeting the WHP and RSRR for calculating the transition process of different GVCSs under four typical water heads. Through example analysis, it is found that two-stage broken line and three-stage delayed GVCS after optimizing the parameters can limit the maximum WHP and RSRR of unit in high-head PSPS. It is obvious that the optimization model of GVCS based on multiobjective NSGA-II is feasible and efficient. Furthermore, the two-stage broken line GVCS has a significant advantage when the unit operates in the high-head range and can achieve the balance of WHP and RSRR. The three-stage delayed GVCS has an obvious effect on limiting the maximum WHP and RSRR of the unit, which is suitable for various water heads, and has large optimization space. However, in practical engineering applications, the three-stage delayed GVCS requires high standard of feedback signal and execution system. Further research and analysis are needed in the improvement of speed governor software and hardware. The research results of this paper can provide scientific guidance for the regulation of GVCS in the initial stage of the construction of PSPS and shorten the commissioning cycle significantly.

Data Availability

The data used in this paper are the unit data of actual pumped storage power station.

Conflicts of Interest

The authors declare that they have no conflicts of interest.

Acknowledgments

This research was supported by the following funding programs: National Natural Science Foundation of China (51809083 and 51809099), Fundamental Research Funds for the Central Universities (2018B48614 and 2019B15114), Natural Science Foundation of Jiangsu Province (BK20180504 and BK20170299), China Postdoctoral Science Foundation (2019M651678), and Water Conservancy Science & Technology Project of Jiangsu Province (2018026). The authors are grateful for support from Dr. Xuyi Peng and Hongpong Pumped Storage Co., Ltd.

References

[1] X. Yuan, X. Wang, and J. Zuo, "Renewable energy in buildings in China—A review," *Renewable and Sustainable Energy Reviews*, vol. 24, pp. 1–8, 2013.

[2] B. G. Mulu, P. P. Jonsson, and M. J. Cervantes, "Experimental investigation of a Kaplan draft tube—Part I: best efficiency point," *Applied Energy*, vol. 93, pp. 695–706, 2012.

[3] Y. Liu, J. Yang, J. Yang et al., "Transient simulations in hydropower stations based on a novel turbine boundary," *Mathematical Problems in Engineering*, vol. 2016, Article ID 1504659, 13 pages, 2016.

[4] R. R. Singh, T. R. Chelliah, and P. Agarwal, "Power electronics in hydro electric energy systems–A review," *Renewable and Sustainable Energy Reviews*, vol. 32, pp. 944–959, 2014.

[5] B. Li, Z. Duan, and J. Wu, "Short-circuit analysis of pumped storage unit during back-to-back starting," *IET Renewable Power Generation*, vol. 9, no. 2, pp. 99–108, 2014.

[6] G. Li, Y. Wang, P. Cao et al., "Effects of the splitter blade on the performance of a pump-turbine in pump mode," *Mathematical Problems in Engineering*, vol. 2018, Article ID 2403179, 10 pages, 2018.

[7] Y. Zhang, Y. Zhang, and Y. Wu, "A review of rotating stall in reversible pump turbine," *Proceedings of the Institution of Mechanical Engineers, Part C: Journal of Mechanical Engineering Science*, vol. 231, no. 7, pp. 1181–1204, 2017.

[8] Y. Zhang, T. Chen, J. Li et al., "Experimental study of load variations on pressure fluctuations in a prototype reversible pump turbine in generating mode," *Journal of Fluids Engineering*, vol. 139, no. 7, Article ID 074501, 2017.

[9] A. Rogeau, R. Girard, and G. Kariniotakis, "A generic GIS-based method for small Pumped Hydro Energy Storage (PHES) potential evaluation at large scale," *Applied Energy*, vol. 197, pp. 241–253, 2017.

[10] W. C. Schleicher and A. Oztekin, "Hydraulic design and optimization of a modular pump-turbine runner," *Energy Conversion and Management*, vol. 93, pp. 388–398, 2015.

[11] D. Beevers, L. Branchini, V. Orlandini, A. De Pascale, and H. Perez-Blanco, "Pumped hydro storage plants with improved operational flexibility using constant speed francis runners," *Applied Energy*, vol. 137, pp. 629–637, 2015.

[12] Z. Zuo, H. Fan, S. Liu et al., "S-shaped characteristics on the performance curves of pump-turbines in turbine mode—A review," *Renewable and Sustainable Energy Reviews*, vol. 60, pp. 836–851, 2017.

[13] D. Li, H. Wang, Y. Qin, L. Han, X. Wei, and D. Qin, "Entropy production analysis of hysteresis characteristic of a pump-turbine model," *Energy Conversion and Management*, vol. 149, pp. 175–191, 2017.

[14] J. Zhou, Y. Xu, Y. Zheng et al., "Optimization of guide vane closing schemes of pumped storage hydro unit using an enhanced multi-objective gravitational search algorithm," *Energies*, vol. 10, no. 7, Article ID 911, 2017.

[15] W. Zeng, J. Yang, J. Hu et al., "Guide-vane closing schemes for pump-turbines based on transient characteristics in S-Shaped region," *Journal of Fluids Engineering*, vol. 138, no. 5, Article ID 051302, 2016.

[16] X. Yu, J. Zhang, and D. Miao, "Innovative closure law for pump-turbines and field test verification," *Journal of Hydraulic Engineering*, vol. 141, no. 3, Article ID 05014010, 2014.

[17] J. Zhang, J. Hu, M. Hu et al., "Study on the reversible pump-turbine closing law and field test," in *Proceedings of the ASME 2006 2nd Joint US-European Fluids Engineering Summer Meeting Collocated With the 14th International Conference on Nuclear Engineering*, pp. 931–936, Washington, DC, USA, July 2006.

[18] T. Kuwabara, K. Katayama, H. Nakagawa et al., "Improvements of transient performance of pump turbine upon load rejection," in *Proceedings of the 2000 Power Engineering Society Summer Meeting*, vol. 3, pp. 1783–1788, Seattle, WA, USA, July 2000.

[19] W. Y. Sao, *Numerical simulation on hydraulic transient with mgv in pumped storage and its application*, Ph.D. thesis, Zhejiang University, Hangzhou, China, 2004.

[20] H. Sun, R. Xiao, W. Liu et al., "Analysis of S characteristics and pressure pulsations in a pump-turbine with misaligned guide vanes," *Journal of Fluids Engineering*, vol. 135, no. 5, Article ID 051101, 2013.

[21] J. Clarke and J. T. McLeskey, "Multi-objective particle swarm optimization of binary geothermal power plants," *Applied Energy*, vol. 138, pp. 302–314, 2015.

[22] W. Hong and M. A. Liang, "Multi-objective particle swarm optimization," *Computer Engineering and Applications*, vol. 145, no. 4, pp. 82–85, 2008.

[23] C. Li, J. Zhou, P. Lu, and C. Wang, "Short-term economic environmental hydrothermal scheduling using improved multi-objective gravitational search algorithm," *Energy Conversion and Management*, vol. 89, pp. 127–136, 2015.

[24] A. Ajami and M. Armaghan, "Application of multi-objective gravitational search algorithm (GSA) for power system stability enhancement by means of STATCOM," *International Review of Electrical Engineering*, vol. 7, no. 4, pp. 4954–4962, 2012.

[25] Y. Zhang, S. Hong, J. Lin, and fnm Zheng, "Influence of ultrasonic excitation sealing on the corrosion resistance of HVOF-sprayed nanostructured WC-CoCr coatings under different corrosive environments," *Coatings*, vol. 9, no. 11, p. 724, 2019.

[26] N. Srinivas and K. Deb, "Muiltiobjective optimization using nondominated sorting in genetic algorithms," *Evolutionary Computation*, vol. 2, no. 3, pp. 221–248, 1994.

[27] K. Deb, A. Pratap, S. Agarwal, and T. Meyarivan, "A fast and elitist multiobjective genetic algorithm: NSGA-II," *IEEE Transactions on Evolutionary Computation*, vol. 6, no. 2, pp. 182–197, 2002.

[28] Y. Zhang, J. Zhang, Y. Zheng et al., "Experimental analysis and evaluation of the numerical prediction of wake characteristics of tidal stream turbine," *Energies*, vol. 10, no. 12, p. 2057, 2017.

[29] Z. Wang, B. Zhu, X. Wang, and D. Qin, "Pressure fluctuations in the s-shaped region of a reversible pump-turbine," *Energies*, vol. 10, no. 1, p. 96, 2017.

[30] M.-A. Xue and P. Lin, "Numerical study of ring baffle effects on reducing violent liquid sloshing," *Computers & Fluids*, vol. 52, pp. 116–129, 2011.

[31] Y. Zhang, Y. Xu, Y. Zheng et al., "Multiobjective optimization design and experimental investigation on the axial flow pump with orthogonal test approach," *Complexity*, vol. 2019, Article ID 1467565, 14 pages, 2019.

[32] M.-A. Xue, J. Zheng, P. Lin, and X. Yuan, "Experimental study on vertical baffles of different configurations in suppressing sloshing pressure," *Ocean Engineering*, vol. 136, pp. 178–189, 2017.

[33] Y. Zhang, C. Li, Y. Xu et al., "Study on propellers distribution and flow field in the oxidation ditch based on two-phase CFD model," *Water*, vol. 11, no. 12, Article ID 2506, 2019.

[34] W. Zang, Y. Zheng, Y. Zhang, J. Zhang, and E. Fernandez-Rodriguez, "Experiments on the mean and integral characteristics of tidal turbine wake in the linear waves propagating with the current," *Ocean Engineering*, vol. 173, pp. 1–11, 2019.